



# Electrical Characterisation of A $\delta$ -Fibres Based on Human *in vivo* Electrostimulation Threshold

Shota Tanaka<sup>1</sup>, Jose Gomez-Tames<sup>1,2</sup>, Toshiaki Wasaka<sup>1,2</sup>, Koji Inui<sup>3,4</sup>, Shoogo Ueno<sup>2,5</sup> and Akimasa Hirata<sup>1,2,6\*</sup>

<sup>1</sup> Department of Electrical and Mechanical Engineering, Nagoya Institute of Technology, Nagoya, Japan, <sup>2</sup> Center of Biomedical Physics and Information Technology, Nagoya Institute of Technology, Nagoya, Japan, <sup>3</sup> Department of Functioning and Disability, Institute for Developmental Research, Aichi Developmental Disability Center, Kasugai, Japan, <sup>4</sup> Department of Integrative Physiology, National Institute for Physiological Sciences, Okazaki, Japan, <sup>5</sup> Department of Biomedical Engineering, Graduate School of Medicine, The University of Tokyo, Tokyo, Japan, <sup>6</sup> Frontier Research Institute for Information Science, Nagoya Institute of Technology, Nagoya, Japan

## OPEN ACCESS

### Edited by:

Michele Giugliano,  
International School for Advanced  
Studies (SISSA), Italy

### Reviewed by:

Aritra Kundu,  
The University of Texas at Austin,  
United States  
Vassily Tsytarev,  
University of Maryland, College Park,  
United States

### \*Correspondence:

Akimasa Hirata  
ahirata@nitech.ac.jp

### Specialty section:

This article was submitted to  
Neural Technology,  
a section of the journal  
Frontiers in Neuroscience

**Received:** 28 July 2020

**Accepted:** 18 November 2020

**Published:** 05 January 2021

### Citation:

Tanaka S, Gomez-Tames J,  
Wasaka T, Inui K, Ueno S and Hirata A  
(2021) Electrical Characterisation  
of A $\delta$ -Fibres Based on Human *in vivo*  
Electrostimulation Threshold.  
Front. Neurosci. 14:588056.  
doi: 10.3389/fnins.2020.588056

Electrical stimulation of small fibres is gaining attention in the diagnosis of peripheral neuropathies, such as diabetes mellitus, and pain research. However, it is still challenging to characterise the electrical characteristics of axons in small fibres (A $\delta$  and C fibres). In particular, *in vitro* measurement for human A $\delta$ -fibre is difficult due to the presence of myelin and ethical reason. In this study, we investigate the *in vivo* electrical characteristics of the human A $\delta$ -fibre to derive strength–duration (S–D) curves from the measurement. The A $\delta$ -fibres are stimulated using coaxial planar electrodes with intraepidermal needle tip. For human volunteer experiments, the S–D curve of A $\delta$ -fibre is obtained in terms of injected electrical current. With the computational analysis, the standard deviation of the S–D curve is mostly attributed to the thickness of the stratum corneum and depth of the needle tip, in addition to the fibre thickness. Then, we derive electrical parameters of the axon in the A $\delta$ -fibre based on a conventional fibre model. The parameters derived here would be important in exploring the optimal stimulation condition of A $\delta$ -fibres.

**Keywords:** strength duration curve, selective stimulation of small fibres, extracellular electric field, electrical analysis in biological tissues, electrical stimulation

## INTRODUCTION

Different receptors and peripheral nerve fibres convey somatosensory information to the central nervous system. Selective stimulation of nerve fibres is essential in observing the activation of a somatosensory submodality system. The rationale for this is based on different conduction velocities of fibres with different thicknesses (Vallbo et al., 1979). The brain responses for first arriving signals may suppress the effect of those for later arriving signals.

Terminals of afferent A $\delta$ - and C-fibres are located in the epidermis. Meanwhile, mechanoreceptors are located in the upper layer of the dermis. Unlike the activation of the touch system, which is characterised by the stimulation of thick A $\beta$  fibres, thin A $\delta$ - or C-fibres can be stimulated in a selective manner for pain system activation. Recent studies used selective stimulation of small fibres in patients suffering from peripheral neuropathies, such as diabetes mellitus (Kukidome et al., 2015; Omori et al., 2017; Suzuki et al., 2020).

There are several techniques for selective stimulation of thin fibres based on the electrophysiological differences among peripheral fibres: radiant heat stimulation by lasers for

A $\delta$ -fibres (Bromm et al., 1983; Bragard et al., 1996; Magerl et al., 1999; Opsommer et al., 2001; Nahra and Plaghki, 2003; Churyukanov et al., 2012) and intraepidermal electrical stimulation (IES) for both C- and A $\delta$ -fibres (Inui et al., 2002).

IES uses a small concentric bipolar needle electrode to inject a current of a few milliamperes to generate a focused electric field around the electrodes (Inui and Kakigi, 2012). Different stimulation conditions have been proposed in applying selective stimulation of A $\delta$ - and C-fibres in different studies: different polarities of electrode, durations, larger interstimulus interval, and waveforms (Inui and Kakigi, 2012; Kodaira et al., 2014; Hugosdottir et al., 2019). The stimulation of A $\delta$ - and C-fibres has been determined based on the latency in the fibres. Thus, optimal stimulation condition for these small fibres is a challenging topic. Except for the diameter, the physical parameters of the fibres are still unknown and controversial (Reilly and Diamant, 2011).

One method used to characterise the fibre response and its electrical characteristics is the strength–duration relationship (S–D curve), which represents the threshold dependence of the pulse duration for electrostimulation. The electrostimulation threshold becomes small with the increase in the pulse durations until converging to a minimum threshold termed “rheobase.” Only two studies have measured perception threshold to derive S–D curves but were not specific to one type of small fibre (co-activation of different small fibres) (Hennings et al., 2017). Recently, Poulsen et al. (2020) investigated S–D curves of A $\delta$ -fibres for different electrodes; the rheobase was estimated in terms of injection current, which is not induced by physical quantity. Moreover, only a few pulse durations were considered. All these experiments are based on *in vivo* experiments and assume activation thresholds of the fibre equal to activation perception sensation in the experiment. This is because they have not yet succeeded in creating the human A $\delta$ -fibres for *in vitro* experiment, because of the presence of myelin. Thus, the rheobase of A $\delta$ -fibres has not been well quantified, except for an empirical estimation (Reilly and Diamant, 2011).

Computational electromagnetics has become a powerful tool in determining the induced electric field for an external field exposure or current injection. To date, only a few studies have been performed using electromagnetic dosimetry in peripheral nerves in the skin (Mørch et al., 2011; Frahm et al., 2013; Hirata et al., 2013a). In our previous study (Motogi et al., 2016), we conducted computational dosimetry of the skin for the injection current to assess nerve stimulation.

The present study aimed to estimate the electrical parameters of A $\delta$ -fibres via comparison of *in vivo* experiment and computation. One of the features of this study is that the computation is based on multiscale stimulation combining electromagnetic dosimetry and nerve activation modelling.

## MATERIALS AND METHODS

### IES Experiment

The experiments in measuring perception threshold through A $\delta$ -fibre stimulation were performed on 14 healthy male subjects (age,  $21.8 \pm 1.7$  years). The experiments were approved by the

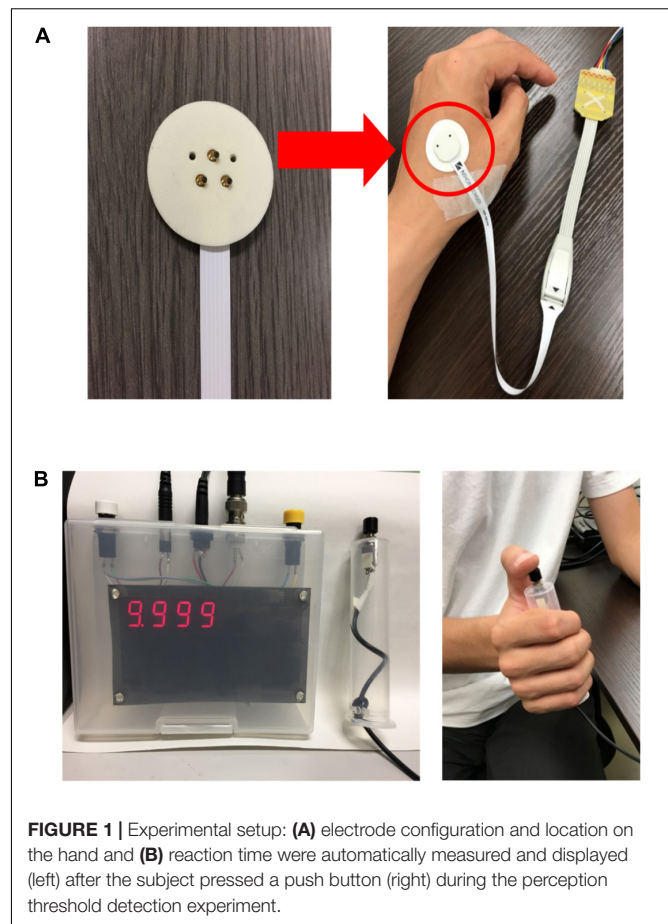
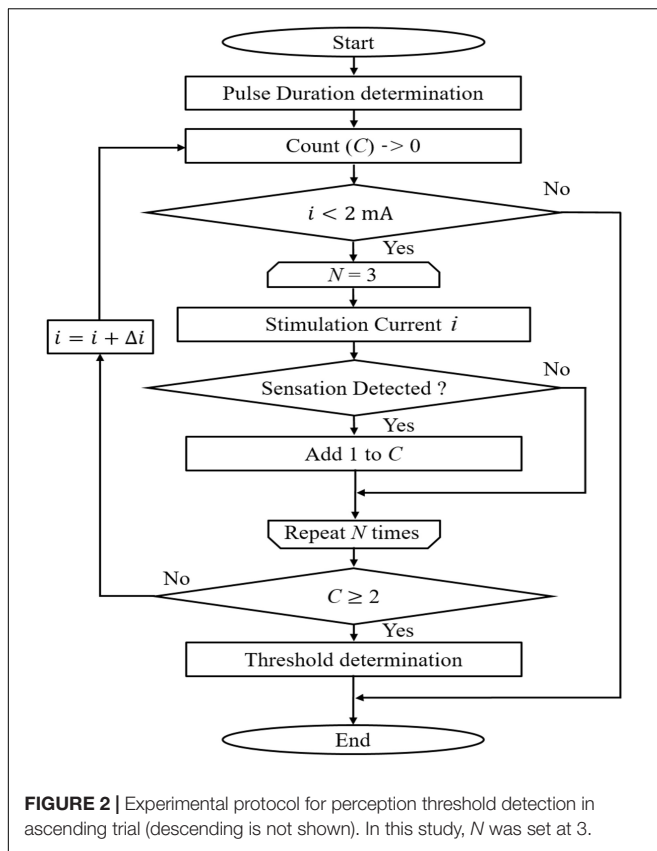


**FIGURE 1** | Experimental setup: (A) electrode configuration and location on the hand and (B) reaction time were automatically measured and displayed (left) after the subject pressed a push button (right) during the perception threshold detection experiment.

Ethical Committee of the Nagoya Institute of Technology. The experimental setup is presented in **Figure 1**. The stimulation device (STG4004, Multi Channel Systems GmbH, Germany) delivered a single square pulse current through a concentric bipolar needle electrode (NM-983 W, Nihon Kohden, Tokyo, Japan). The inner needle and ring electrodes were assigned to the anode and cathode of the stimulation device, respectively. The pulse duration and current intensity were varied during the experiment to explore the threshold. The stimulation was applied to the dorsum of the left hand.

The experimental protocol to measure the perception threshold (defined as the lowest injection current at which the subject feels a sensation) is shown in **Figure 2**. The subjects were instructed to press a button as soon as they felt the minimum sensation. The time between stimulation onset and detection by pressing a button (termed reaction time) was automatically recorded. The method of limits was used to determine the stimulus threshold with consecutive ascending and descending trials. A total of six trials were performed per subject. For ascending trials, the injection current intensity was increased in steps of 0.05 mA. Each session of the ascending trial consisted of  $N$  consecutive stimulations with the same current intensity and fixed stimulation duration, in which the stimulations were delivered at an undisclosed time to the subject. We set  $N$  to 3 to obtain a reliable perception threshold in a set. The threshold



was considered detected when the subject reported a sensation at least two of three times with reaction time in the range of A $\delta$ -fibre transmission (200–800 ms) (Rag e et al., 2010; Kodaira et al., 2014). The rest time between sets of three stimulations was 1 min to reduce the effect of habituation. If a maximum limit of 2 mA was reached, the perception threshold was considered as not found. For descending trials, the current intensity was decreased by 0.05 mA until the stimulus was not detected. The mean of the six trials was obtained as the stimulus threshold. Six sessions were conducted for different pulse durations (60, 100, 200, 400, 800, and 1600  $\mu$ s), which were randomly selected. The rest time between three stimulation sets was also 1 min to reduce the effect of habituation.

## Modelling Needle Electrodes and the Skin

Our IES model was almost identical to that in our previous study (Motogi et al., 2016). In brief, the concentric bipolar needle electrode used in the experiment is modelled as shown in **Figure 3A** (Motogi et al., 2014). The inner electrode and ring electrode corresponded to the cathode and anode, respectively, and modelled as a perfect conductor. The part of the inner needle protruding from the outer ring (called  $d_N$  ‘needle depth’ hereafter) was selected between 5 to 30  $\mu$ m for experiments mentioned in section ‘‘Computational Estimation of Electric Field in the Skin Model’’ and fixed to 20  $\mu$ m in section ‘‘Development of Computational A $\delta$ -Fibre Model’’.

The skin was modelled as a layered structure for hairy skin (Alekseev and Ziskin, 2007; Schmid et al., 2013; De Santis et al., 2015; Motogi et al., 2016). The thickness of the stratum corneum layer was 10–20  $\mu$ m. The boundary between the epidermis and dermis layers was treated as a transition region (10–30  $\mu$ m). The epidermis thickness was reported as 50–70  $\mu$ m (Valentin, 2002; Koster et al., 2012). The corresponding conductivities values are shown in **Figure 3B**. In detail, the conductivity of the stratum corneum was selected as  $2 \times 10^{-4}$  [S/m] at 2.1 kHz based on Gabriel et al. (1996). In the transit region between the epidermis and dermis, the variation of the conductivity was approximately proportional to the water content (Faes et al., 1999; Egawa and Kajikawa, 2009). The conductivity of the dermis at sufficient depth was 0.21 S/m based on Sasaki et al. (2016).

The dimensions of the skin model were 1.54 mm (depth)  $\times$  1.65 mm  $\times$  1.65 mm and discretised by voxels of 5  $\mu$ m of length. We confirmed no variation of the electric field if larger dimensions are used as the current flow is confined between the electrodes.

## Volume Conductor Model of Skin

The electrical skin model is treated as a passive volume conductor to compute the *in situ* electric field produced by the injected current considering that the frequency is below kilohertz range and displacement current is negligible (Hirata et al., 2013b). The effects of the electric fields generated by neural activity was ignored.

The scalar potential finite difference method (Dawson and Stuchly, 1996) is used to numerically solve the following equation to obtain the scalar potential  $\phi$ :

$$\nabla \cdot (\sigma \nabla (\phi)) \quad (1)$$

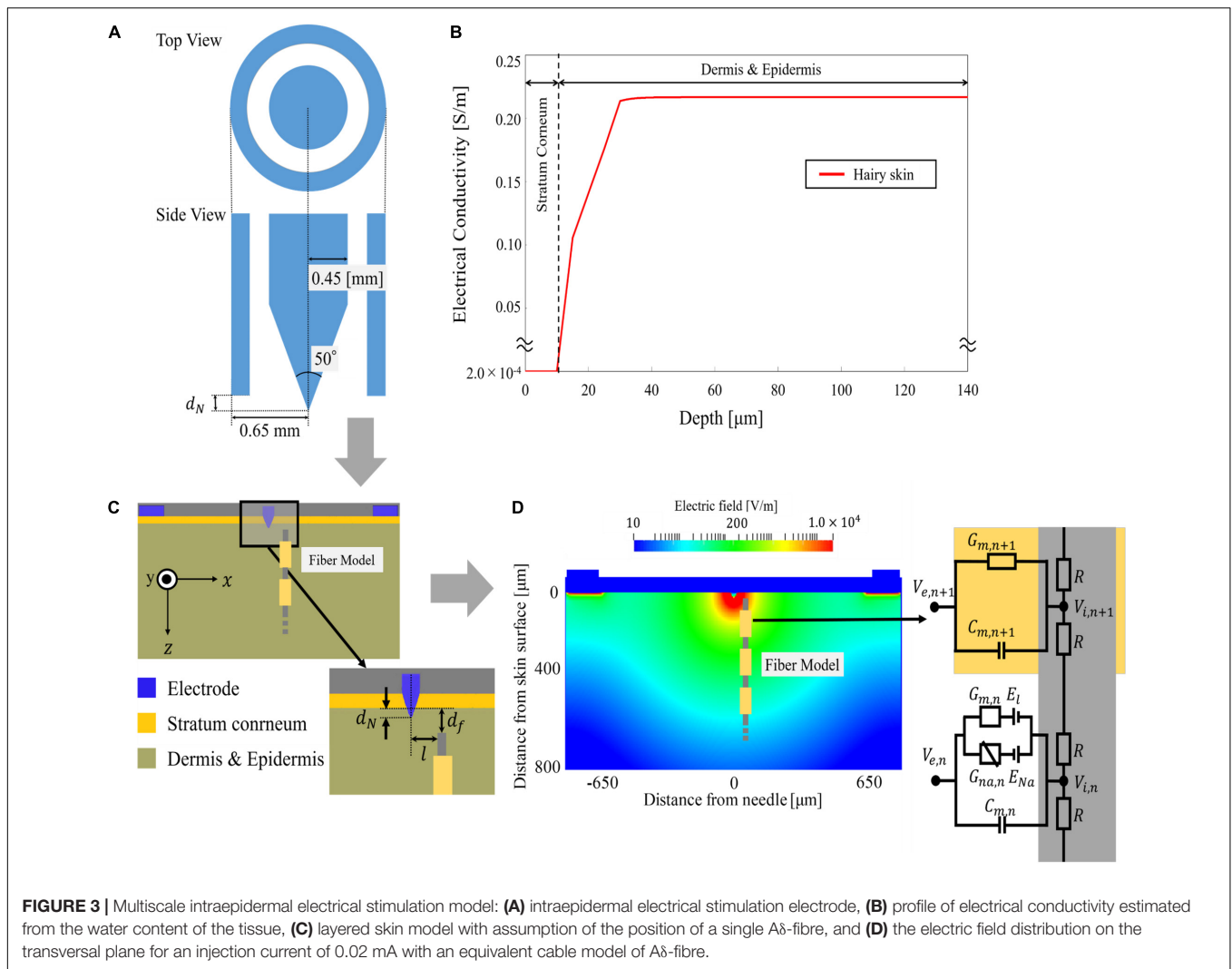
where  $\sigma$  denotes the tissue conductivity. The potential was solved iteratively using the successive-over-relaxation and multigrid methods (Laakso and Hirata, 2012). A current source was connected between the inner electrode and outer ring of the electrode. To obtain the *in situ* electric field, the potential difference between nodes of the voxel was divided by the voxel length. The injection current to generate an electric field distribution that can depolarise a fibre and generate an action potential was computed in the following section.

## Nerve Activation Modelling for A $\delta$ -fibre

The effects of the extracellular electric field derived from Eq. (1) on a myelinated nerve fibres were described using the following general equation (McNeal, 1976; Rattay, 1999):

$$\begin{aligned} C_{m,n} \frac{dV_{m,n}}{dt} + I_{ion,n} - \frac{V_{m,n-1} - 2V_{m,n} - 2V_{m,n+1}}{0.5 (R_{m,i} + R_{m,n})} \\ = \frac{V_{e,n-1} - 2V_{e,n} - 2V_{e,n+1}}{0.5 (R_{m,i} + R_{m,n})} \end{aligned} \quad (2)$$

where  $C_m$  is the membrane capacitance and  $R_{m,i}$  and  $R_{m,n}$  are the internode membrane resistivity and nodal membrane resistivity, respectively. The membrane potential is represented by the variable  $V_{m,n} = V_e - V_i$ . The fibres are formed by internodes



(myelin segments) and nodes of Ranvier (ionic channels) as shown in **Figure 3D**. At the internodes, the membrane current  $I_{ion,n}$  was modelled by the passive conductance ( $G_{m,n}$ ) multiplied by the membrane potential. At the nodes of Ranvier, the ionic membrane current was formulated using the Chiu–Ritchie–Rogart–Stagg–Sweeney model (CRRSS), which is a conductance-based voltage-gated model (Sweeney et al., 1987). Here, the ionic current follows

$$I_{ion,n} = G_{Na}m^3h(V_{m,n} - E_{Na}) + G_L(V_{m,n} - E_L) \quad (3)$$

where  $G_L$  and  $G_{Na}$  are the leak passive conductance and sodium channel conductance, respectively, and  $E_{Na}$  and  $E_L$  are the reversal potentials. Sodium channel activation and inactivation are controlled by the dimensionless variables  $m$  and  $h$ .

The smallest injection current to propagate an action potential in an axon was obtained (called activation threshold) using a search method (bisection method) (Gomez-Tames et al., 2018) until the error was smaller than 10  $\mu$ A. An action potential was elicited when the membrane potential was depolarised up to 80 mV in at least four neighbouring nodes at successive times

(Reilly, 2016). It is reasonable to apply a similar algorithm to central nervous tissue when the target is direct stimulation of pyramidal tracts.

### S–D Curve

The S–D curve is the relationship between the activation threshold and pulse duration. Two metrics were derived for the S–D curve: rheobase and chronaxie. However, unlike *in vitro* studies, we defined threshold as the perception threshold instead of activation threshold. Because the perception was caused by synaptic mechanism of the peripheral and central nervous systems, actual threshold of activation of a single fibre would be smaller than that reported in this study.

Rheobase is the minimum current intensity that elicits an activation that occurs after a long duration, and chronaxie is the time when stimulation current is twice the rheobase. The mathematical expression for the S–D curve was as follows:

$$I = b(1 + C/w) \quad (4)$$

**TABLE 1** | Coefficient of variation in measured results and its normalised value by rheobase.

Pulse width ( $\mu$ s)	Coefficient of variation	
	Non-normalised	Normalised
60	0.30	0.37
100	0.36	0.34
200	0.42	0.37
400	0.38	0.22
800	0.50	0.16
1600	0.33	0.18

where  $I$  is the input current,  $b$  is the rheobase,  $c$  is the chronaxie, and  $w$  is the pulse width. These parameters described the excitability characteristics of different nerve fibres. The effect of electrical parameters in the circuit model on rheobase and chronaxie was examined.

## Nerve Parameters

The A $\delta$ -fibre diameter ( $D$ ) was in the range of 0.68–1.46  $\mu$ m, with an average of  $1.08 \pm 0.15$   $\mu$ m (Reilly et al., 1997). The depth from the skin surface ( $d_f$ ) of A $\delta$ -fibre was between 10 and 40  $\mu$ m (MacIver and Tanelian, 1993). In this study, to fit the experimental S–D curve, the diameter of the fibre model was fixed to  $D = 1.0$   $\mu$ m and  $d_f = 25$   $\mu$ m (Figure 3C).

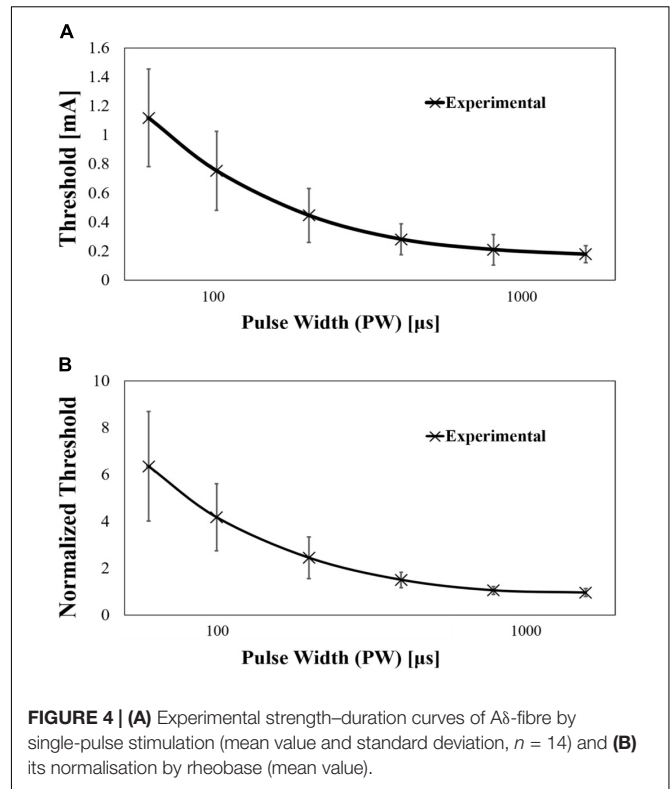
The nerve fibre model for activation was based on the CRRSS model, and then the parameters in the model were explored. The electrical parameters of the CRRSS model are shown in the **Supplementary Table 1**. The fibre model was initially placed at  $l = 0.25, 0.30,$  and  $0.35$  mm. This was because the subjects could feel the sensation originated when multiple nerves were stimulated and integrated. The experimental values were considered to be the thresholds of the nerve located farthest from the electrode among multiple nerves that were stimulated. Second, the  $C$  and  $G_l$  parameters were modified from the original values to adjust the chronaxie value (Sweeney et al., 1987). We adopted the least squares error for each pulse width to adjust the chronaxie. The electrical parameters used in the modified CRRSS model are listed in **Table 1**.

Note that these fibres and electrode/skin spatial parameters are closely related to each other and thus should be fitted in an iterative manner. However, for simplicity, the spatial distance  $l$  was fixed, as mentioned above, and then the remaining fibre parameters are shown. The presented results are results of three iterations.

## EXPERIMENTAL AND COMPUTATIONAL RESULTS

### Experiment Results of A $\delta$ -Fibre

The current amplitude of A $\delta$ -fibre for a single pulse injection was obtained experimentally, as shown in **Figure 4A**. The mean rheobase and chronaxie were 0.178 mA [standard deviation (SD) of 0.057 mA] and 270  $\mu$ s (SD of 120  $\mu$ s), respectively. As will

**FIGURE 4** | (A) Experimental strength–duration curves of A $\delta$ -fibre by single-pulse stimulation (mean value and standard deviation,  $n = 14$ ) and (B) its normalisation by rheobase (mean value).**TABLE 2** | Reaction time during sensation threshold detection experiment.

Pulse width ( $\mu$ s)	Reaction time (s) (Mean $\pm$ SD)
60	0.496 $\pm$ 0.100
100	0.500 $\pm$ 0.103
200	0.519 $\pm$ 0.102
400	0.521 $\pm$ 0.090
800	0.493 $\pm$ 0.085
1600	0.470 $\pm$ 0.092

be discussed later, a part of the variability of the rheobase was attributed to the morphology of the skin and depth of the needle tip. Thus, the measured threshold of A $\delta$ -fibre was normalised by rheobase (Figure 4B). The normalised chronaxie was 277  $\mu$ s (SD of 118  $\mu$ s). Then, we evaluated the coefficient of variation (CoV) of measured rheobases and its normalised values (Table 1). The CoV is the standard deviation divided by the average value. From Table 1, the CoV for measured value was not significantly affected by pulse width. However, the CoV for the normalised results was smaller than those without normalisation and more variable for short pulse width.

The reaction time of the volunteers is shown in Table 2. The reaction time was stable along the experiment with a maximum variation of 5%, which was consistent with those in previous studies (Kodaira et al., 2014).

**TABLE 3** | Combined effect of the needle depth and thickness of the stratum corneum on the position  $l = 0-0.35$  of the electric field (mean value and standard deviation).

Depth of the needle electrode ( $\mu\text{m}$ )	Electric field strength (V/m)	
	Mean $\pm$ SD	Max
5	3692.3 $\pm$ 4023.7	18,195.0
10	3761.6 $\pm$ 4190.9	19,824.9
15	3780.9 $\pm$ 4236.9	20,927.4
20	3892.2 $\pm$ 4525.7	24,322.6
30	4191.2 $\pm$ 5407.9	37,029.6

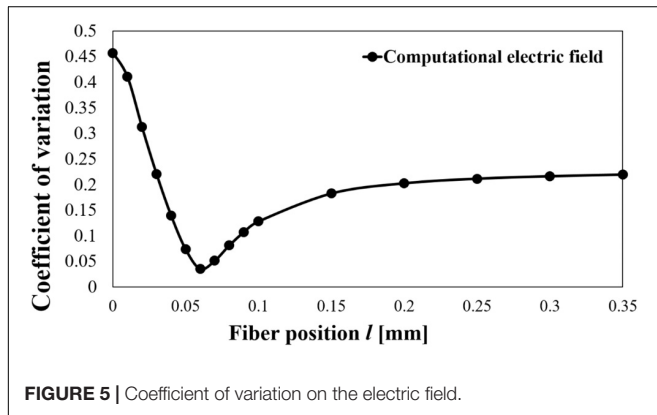


**FIGURE 5** | Coefficient of variation on the electric field.

## Model Variability Effect

### Computational Estimation of Electric Field in the Skin Model

The effect of the needle electrode and stratum corneum layer on the electric field is shown in **Table 3**. In the skin model, the depth of the needle electrode was varied at 5, 10, 15, 20, and 30  $\mu\text{m}$  from the skin surface, and the stratum corneum thickness was 5, 10, 15, or 20  $\mu\text{m}$ . Considering the characteristics and number of A $\delta$ -fibre, the position of the electric field was selected as  $l = 0-0.35$  mm, and the depth at each position was  $d_f = 10-40$   $\mu\text{m}$  (steps of 5  $\mu\text{m}$ ) based on the ending of the fibre (MacIver and Tanelian, 1993).

The injection current was set as 20  $\mu\text{A}$ . The induced electric field at the end of the fibre was computed, considering all combinations of the depth of the needle electrode and stratum corneum (total 20 cases). However, the computational result for the models whose electrode depth is 5  $\mu\text{m}$  and stratum corneum is 20  $\mu\text{m}$  was excluded. The reason for this exclusion was computational instability, which is attributable to the stratum corneum thickness; the electric current may not flow with low conductivity of the stratum corneum. **Table 3** shows that the stronger the electric field at the end of the fibre, the deeper the needle electrode.

Then, we evaluated the CoV of the electric field strength for all models using the previous parameters (**Figure 5**). **Figure 5** shows that the CoV was more variable close to the needle electrode and minimum value at  $l = 0.06$  mm. We varied the fibre diameter  $D$  at 0.68, 0.80, 1.0, 1.2, or 1.46  $\mu\text{m}$  (Reilly et al., 1997). Assuming that the stimulation threshold of the fibres was inversely proportional

**TABLE 4** | Estimated parameters based on the measured results (see Section “Experiment Results of A $\delta$ -Fibre”).

Parameter	Original parameters	Value		
		$l = 0.25$ mm	$l = 0.30$ mm	$l = 0.35$ mm
Capacity of membrane (C)	28.8 nF	26.4 times	20.0 times	12.0 times
Leaked channel conductivity ( $G_l$ )	128 mS/cm <sup>2</sup>	0.25 times	0.14 times	0.27 times
Rheobase		0.183 mA	0.169 mA	0.161 mA
Chronaxie		247 $\mu\text{s}$	273 $\mu\text{s}$	280 $\mu\text{s}$

to the nerve diameter, the threshold may vary from 0.68 to 1.46 for the abovementioned parameters. The variation of CoV on the position  $l = 0-0.35$  mm of computational electric field strength was 0.04–0.46. Considering this combined variability, this may mostly explain the variability of the measured results (CoV) in the rheobase (see Section “Experiment Results of A $\delta$ -Fibre”).

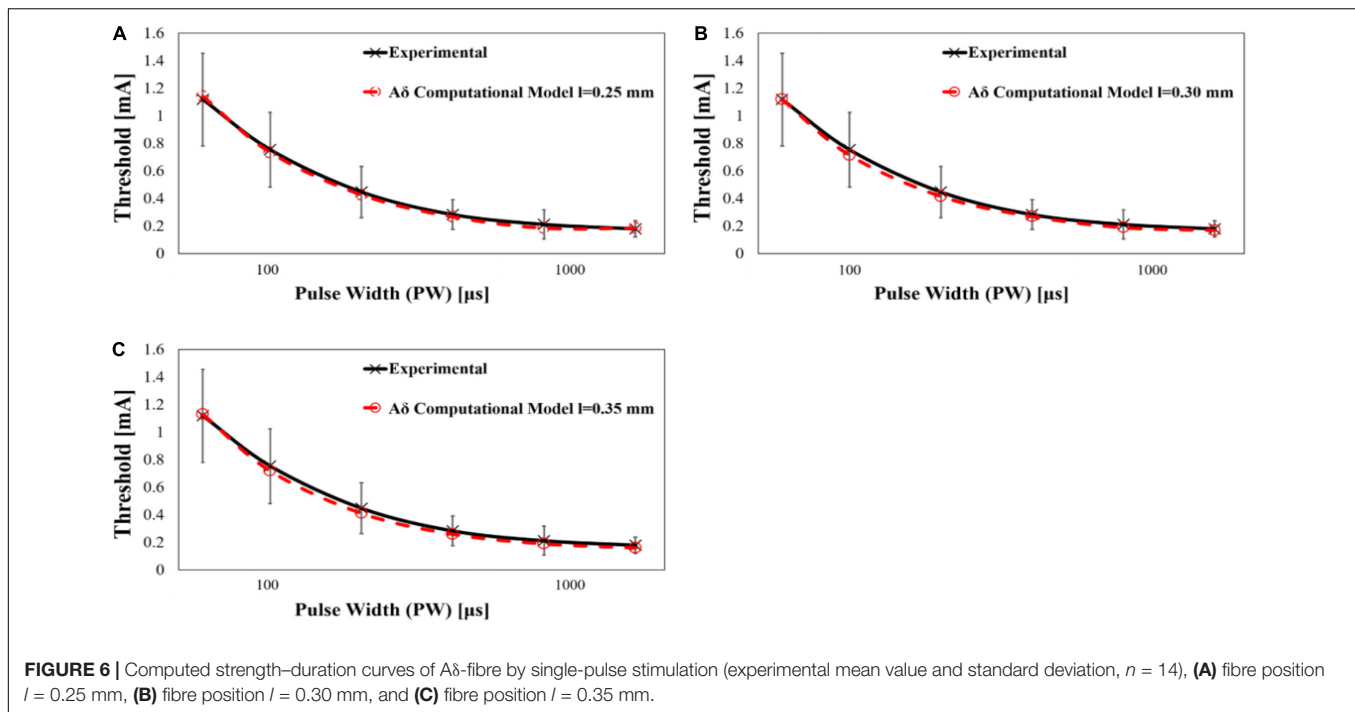
### Development of Computational A $\delta$ -Fibre Model

The electrical parameters of nerve activation model were searched so as to coincide with the experimental data. The least squares error between the experimental and computational results was adopted. We changed  $C$  and  $G_l$  for the electrical parameters in the CRRSS model. For the estimated parameters based on the measured results, the corresponding parameters of  $C$  and  $G_l$  are shown in **Table 4**. The electrical parameters used in the modified CRRSS model are shown in **Table 4** (refer to **Supplementary Table 1** for more details). Note that the parameters in the CRRSS model were derived from the measurement of the rabbit muscle (Chiu and Ritchie, 1980).

The computational results of A $\delta$ -fibre are shown in **Figure 6**, and the parameters of rheobase and chronaxie are shown in **Table 4**. Also, the rheobase of computed electric field strength at the end of fibre ( $d_f = 10-40$   $\mu\text{m}$ ) was 262.8–500.4 V/m at  $l = 0.25$  mm, 128.9–249.0 V/m at  $l = 0.30$  mm, and 66.4–129.4 V/m at  $l = 0.35$  mm. The difference between mean experiment and modelled rheobase was 2.98–10.1%. Meanwhile, the difference between the chronaxie values was 1.22–8.52%.

## DISCUSSION

Nociceptive A $\delta$ -fibre is one type of cutaneous sensory neurons. The terminal of A $\delta$ -fibres is found in the epidermis (Kandel et al., 2012). In this study, an experiment for selective stimulation of A $\delta$ -fibre was conducted with the IES targeting them. The activation threshold of A $\delta$ -fibre is characterised by the S–D curve using single-pulse stimulation. Then, an A $\delta$ -fibre model is derived based on experimentally derived S–D curve. The CoV in the measured threshold was more varied for brief pulse injection. One of the possibilities for this is that the ending of the A $\delta$ -fibre is unmyelinated. The difference in the myelin thickness influenced the amount of charge stored in the fibre, so the variation in the short pulse width was large. The chronaxie was estimated in a recent study (Poulsen et al., 2020) as 599–756  $\mu\text{s}$ ,



which is twice larger than that in our study. However, only four different durations (0.1, 0.5, 1, and 10 ms) were considered in that study. Moreover, our axon model is an extension of the CRRSS model, whereas their own proposal was based on their previous study by Tigerholm et al. (2019).

One difference of this S–D curve was that it was characterised by the injection current, which is not an *in situ* parameter and affected by the stimulator. Then, we conducted computational estimation of electrical parameters of A $\delta$ -fibre based on the CRRSS model. The CoV on the computational electric field where the nerve ending was ranged from 0.04 to 0.45. Combining potential variability of fibre thickness, most experimental variations can be explained. Also, the rheobase value in terms of the internal electric field strength at the fibre terminal ( $d_f = 10$ – $40$   $\mu$ m) ranged from 66.4 to 129.4 V/m at  $l = 0.35$  mm. In previous studies, the reported rheobase values were 6.15 V/m using the SENN model (fibre diameter = 20  $\mu$ m) for electrical peripheral nerve stimulation (Reilly and Diamant, 2011) and 5.9 V/m for magnetic stimulation in the forearm (Havel et al., 1997). In this study, the internal electric field threshold was computed for a fibre diameter model of 1.0  $\mu$ m, which corresponds, as expected, to a threshold that is inversely proportional to the diameter of the fibre in peripheral nerve fibres.

The original CRRSS model had a chronaxie value 14 times smaller than that of the experimental chronaxie value. Then, we tuned parameters by fitting the chronaxie of computational results in the CRRSS model to that of experimental results. Increasing  $C$  had an influence on the time to reach the threshold. As a result, when the pulse duration was short, the amount of change in the threshold for pulse duration increased; that is, the chronaxie of computational results increased. In addition, the chronaxie of computational results was simulated in more

detail by making  $G_l$  small. Therefore, we confirmed that the experimental results could be simulated in more detail based on the conventional CRRSS model.

As we estimate the number of fibres, the computed rheobase was adjusted by changing the fibre position  $l$  for each diameter  $D$  (**Supplementary Figure 1**). The number of fibres was estimated from the fibre position  $l$ , and the A $\delta$ -fibre density was 160 fibres/mm<sup>2</sup> (Ebenezer et al., 2007). In the numerical analysis, it is possible that 31.4 to 61.5 fibres ( $l = 0.25$ – $0.35$  mm) are stimulated by the IES experiment, while considering the variability of needle depth and depth of the fibres. However, in our investigation, it was not possible to conclude how many fibres are activated by the stimulation; as always, multiple fibres are stimulated. Based on Mouraux et al. (2012), the number of activated A $\delta$ -fibres required to elicit a conscious response was estimated as 59. Therefore, the electrical parameters were searched so as to coincide with the experimental data in fibre position  $l = 0.34$  mm (the number of fibres was 59). As a result, the corresponding parameters of  $C$  and  $G_l$  were 13.3 times and 0.34 times, respectively. The rheobase and chronaxie were 0.189 mA and 231  $\mu$ s, respectively.

Uncertainty in the electromagnetic computational analysis is originated, in large part, from the assignment of electrical conductivity values to each tissue (Motogi et al., 2016). In particular, the reliability of the electric field computation in the stratum corneum is affected by non-linear characteristics of the conductivity for fields exceeding the order of kV/m (Yamamoto and Yamamoto, 1981). We can observe that the field strength could reach the dielectric breakdown, but unlikely owing to the non-linearity of the conductivity, as shown in **Figure 5**. On the other hand, the influence of the electrode radius was small.

## DATA AVAILABILITY STATEMENT

The raw data supporting the conclusions of this article will be made available by the authors, without undue reservation.

## ETHICS STATEMENT

The studies involving human participants were reviewed and approved by the Ethical Committee of Nagoya Institute of Technology. The patients/participants provided their written informed consent to participate in this study.

## AUTHOR CONTRIBUTIONS

AH and TW conceived and designed the research. TW and ST conducted the experiments. JG-T and ST conducted

the experiments and processed the data. All authors analysed the data, wrote the manuscript, and read and approved the manuscript.

## FUNDING

This work was supported by the Ministry of Internal Affairs and Communications (Grant Number JPMI10001).

## SUPPLEMENTARY MATERIAL

The Supplementary Material for this article can be found online at: <https://www.frontiersin.org/articles/10.3389/fnins.2020.588056/full#supplementary-material>

## REFERENCES

- Alekseev, S., and Ziskin, M. (2007). Human skin permittivity determined by millimeter wave reflection measurements. *Bioelectromagnetics* 28, 331–339. doi: 10.1002/bem.20308
- Bragard, D., Chen, A., and Plaghki, L. (1996). Direct isolation of ultra-late (C-fibre) evoked brain potentials by CO<sub>2</sub> laser stimulation of tiny cutaneous surface areas in man. *Neurosci. Lett.* 209, 81–84. doi: 10.1016/0304-3940(96)12604-5
- Bromm, B., Neitzel, H., Tecklenburg, A., and Treede, R.-D. (1983). Evoked cerebral potential correlates of C-fibre activity in man. *Neurosci. Lett.* 43, 109–114. doi: 10.1016/0304-3940(83)90137-4
- Chiu, S., and Ritchie, J. (1980). Potassium channels in nodal and internodal axonal membrane of mammalian myelinated fibres. *Nature* 284, 170–171. doi: 10.1038/284170a0
- Churyukanov, M., Plaghki, L., Legrain, V., and Mouraux, A. (2012). Thermal detection thresholds of A $\delta$ - and C-fiber afferents activated by brief CO<sub>2</sub> laser pulses applied onto the human hairy skin. *PLoS One* 7:e35817. doi: 10.1371/journal.pone.0035817
- Dawson, T. W., and Stuchly, M. A. (1996). Analytic validation of a three-dimensional scalar-potential finite-difference code for low-frequency magnetic induction. *Appl. Comput. Electromagn.* 11, 72–81.
- De Santis, V., Chen, X. L., Laakso, I., and Hirata, A. (2015). An equivalent skin conductivity model for low-frequency magnetic field dosimetry. *Biomed. Phys. Eng. Express* 1:015201. doi: 10.1088/2057-1976/1/1/015201
- Ebenezer, G. J., Hauer, P., Gibbons, C., McArthur, J. C., and Polydefkis, M. (2007). Assessment of epidermal nerve fibers: a new diagnostic and predictive tool for peripheral neuropathies. *J. Neuropathol. Exper. Neurol.* 66, 1059–1073. doi: 10.1097/nen.0b013e31815c8989
- Egawa, M., and Kajikawa, T. (2009). Changes in the depth profile of water in the stratum corneum treated with water. *Skin Res. Tech.* 15, 242–249. doi: 10.1111/j.1600-0846.2009.00362.x
- Faes, T., Van der Meij, H., De Munck, J., and Heethaar, R. (1999). The electric resistivity of human tissues (100 Hz–10 MHz): a meta-analysis of review studies. *Physiol. Measur.* 20:R1. doi: 10.1088/0967-3334/20/4/201
- Frahm, K. S., Mørch, C. D., Grill, W. M., Lubock, N. B., Hennings, K., and Andersen, O. K. (2013). Activation of peripheral nerve fibers by electrical stimulation in the sole of the foot. *BMC Neurosci.* 14:116. doi: 10.1186/1471-2202-14-116
- Gabriel, S., Lau, R. W., and Gabriel, C. (1996). The dielectric properties of biological tissues: III. Parametric models for the dielectric spectrum of tissues. *Phys. Med. Biol.* 41, 2271–2293. doi: 10.1088/0031-9155/41/11/003
- Gomez-Tames, J., Kutsuna, T., Tamura, M., Muragaki, Y., and Hirata, A. (2018). Intraoperative direct subcortical stimulation: comparison of monopolar and bipolar stimulation. *Phys. Med. Biol.* 63:225013. doi: 10.1088/1361-6560/aaea06
- Havel, W., Nyenhuis, J., Bourland, J., Foster, K., Geddes, L., Graber, G., et al. (1997). Comparison of rectangular and damped sinusoidal dB/dt waveforms in magnetic stimulation. *IEEE Trans. Magn.* 33, 4269–4271. doi: 10.1109/20.619732
- Hennings, K., Frahm, K. S., Petrini, L., Andersen, O. K., Arendt-Nielsen, L., and Mørch, C. D. (2017). Membrane properties in small cutaneous nerve fibers in humans. *Muscle Nerve* 55, 195–201. doi: 10.1002/mus.25234
- Hirata, A., Hattori, J., Laakso, I., Takagi, A., and Shimada, T. (2013a). Computation of induced electric field for the sacral nerve activation. *Phys. Med. Biol.* 58, 7745–7755. doi: 10.1088/0031-9155/58/21/7745
- Hirata, A., Ito, F., and Laakso, I. (2013b). Confirmation of quasi-static approximation in SAR evaluation for a wireless power transfer system. *Phys. Med. Biol.* 58:N241. doi: 10.1088/0031-9155/58/17/N241
- Hugosdottir, R., Mørch, C. D., Andersen, O. K., and Arendt-Nielsen, L. (2019). “Electrical stimulation of small cutaneous nerve fibers for investigating human pain mechanisms,” in *Proceedings of the Nordic Baltic Conference on Biomedical Engineering and Medical Physics (NBC)*, Reykjavik.
- Inui, K., and Kakigi, R. (2012). Pain perception in humans: use of intraepidermal electrical stimulation. *J. Neurol. Neurosurg. Psychiatry* 83, 551–556. doi: 10.1136/jnnp-2011-301484
- Inui, K., Tran, T. D., Hoshiyama, M., and Kakigi, R. (2002). Preferential stimulation of A $\delta$  fibers by intra-epidermal needle electrode in humans. *Pain* 96, 247–252. doi: 10.1016/S0304-3959(01)00453-5
- Kandel, E. R., Schwartz, J. H., and Jessell, T. M. (2012). *Principles of Neural Science*, 5th Edn, New York, NY: McGraw-Hill.
- Kodaira, M., Inui, K., and Kakigi, R. (2014). Evaluation of nociceptive A $\delta$ - and C-fiber dysfunction with lidocaine using intraepidermal electrical stimulation. *Clin. Neurophysiol.* 125, 1870–1877. doi: 10.1016/j.clinph.2014.01.009
- Koster, I., Loomis, C., Koss, T., and Chu, D. (2012). “Skin development and maintenance,” in *Dermatology*, eds J. Bologna, J. Jorizzo, and J. Schafer (Saunders, PA: Elsevier).
- Kukidome, D., Nishikawa, T., Sato, M., Igata, M., Kawashima, J., Shimoda, S., et al. (2015). Measurement of small fibre pain threshold values for the early detection of diabetic polyneuropathy. *Diabetic Med.* 33, 62–69. doi: 10.1111/dme.12797
- Laakso, I., and Hirata, A. (2012). Fast multigrid-based computation of the induced electric field for transcranial magnetic stimulation. *Phys. Med. Biol.* 57, 7753–7765. doi: 10.1088/0031-9155/57/23/7753
- MacIver, M., and Tanelian, D. L. (1993). Structural and functional specialization of A delta and C fiber free nerve endings innervating rabbit corneal epithelium. *J. Neurosci.* 13, 4511–4524. doi: 10.1523/JNEUROSCI.13-10-04511.1993
- Magerl, W., Ali, Z., Ellrich, J., Meyer, R. A., and Treede, R.-D. (1999). C- and A $\delta$ -fiber components of heat-evoked cerebral potentials in healthy human subjects. *Pain* 82, 127–137. doi: 10.1016/S0304-3959(99)00061-5
- McNeal, D. R. (1976). “Analysis of a model for excitation of myelinated nerve,” in *Proceedings of the IEEE Transactions on Biomedical Engineering*, Piscataway, NJ. doi: 10.1109/TBME.1976.324593
- Mørch, C. D., Hennings, K., and Andersen, O. K. (2011). Estimating nerve excitation thresholds to cutaneous electrical stimulation by finite element

- modeling combined with a stochastic branching nerve fiber model. *Med. Biol. Eng. Comput.* 49, 385–395. doi: 10.1007/s11517-010-0725-8
- Motogi, J., Kodaira, M., Muragaki, Y., Inui, K., and Kakigi, R. (2014). Cortical responses to C-fiber stimulation by intra-epidermal electrical stimulation: an MEG study. *Neurosci. Lett.* 570, 69–74. doi: 10.1016/j.neulet.2014.04.001
- Motogi, J., Sugiyama, Y., Laakso, I., Hirata, A., Inui, K., Tamura, M., et al. (2016). Why intra-epidermal electrical stimulation achieves stimulation of small fibres selectively: a simulation study. *Phys. Med. Biol.* 61:4479. doi: 10.1088/0031-9155/61/12/4479
- Mouraux, A., Rage, M., Bragard, D., and Plaghki, L. (2012). Estimation of intraepidermal fiber density by the detection rate of nociceptive laser stimuli in normal and pathological conditions. *Clin. Neurophysiol.* 42, 281–291. doi: 10.1016/j.neucli.2012.05.004
- Nahra, H., and Plaghki, L. (2003). The effects of A-fiber pressure block on perception and neurophysiological correlates of brief non-painful and painful CO<sub>2</sub> laser stimuli in humans. *Eur. J. Pain* 7, 189–199. doi: 10.1016/S1090-3801(02)00099-X
- Omori, S., Iose, S., Misawa, S., Watanabe, K., Sekiguchi, Y., Shibuya, K., et al. (2017). Pain-related evoked potentials after intraepidermal electrical stimulation to A $\delta$  and C fibers in patients with neuropathic pain. *Neurosci. Res.* 121, 43–48. doi: 10.1016/j.neures.2017.03.007
- Opsommer, E., Weiss, T., Miltner, W., and Plaghki, L. (2001). Scalp topography of ultralate (C-fibres) evoked potentials following thulium YAG laser stimuli to tiny skin surface areas in humans. *Clin. Neurophys.* 112, 1868–1874. doi: 10.1016/S1388-2457(01)00622-8
- Poulsen, A. H., Tigerholm, J., Meijs, S., Andersen, O. K., and Mørch, C. D. (2020). Comparison of existing electrode designs for preferential activation of cutaneous nociceptors. *J. Neural Eng.* 17:036026. doi: 10.1088/1741-2552/ab85b1
- Rag e, M., Van Acker, N., Facer, P., Shenoy, R., Knaapen, M. W., Timmers, M., et al. (2010). The time course of CO<sub>2</sub> laser-evoked responses and of skin nerve fibre markers after topical capsaicin in human volunteers. *Clin. Neurophysiol.* 121, 1256–1266. doi: 10.1016/j.clinph.2010.02.159
- Rattay, F. (1999). The basic mechanism for the electrical stimulation of the nervous system. *Neuroscience* 89, 335–346. doi: 10.1016/S0306-4522(98)00330-3
- Reilly, D., Ferdinando, D., Johnston, C., Shaw, C., Buchanan, K., and Green, M. (1997). The epidermal nerve fibre network: characterization of nerve fibres in human skin by confocal microscopy and assessment of racial variations. *Br. J. Dermatol.* 137, 163–170. doi: 10.1046/j.1365-2133.1997.18001893.x
- Reilly, J. P. (2016). Survey of numerical electrostimulation models. *Phys. Med. Biol.* 61, 4346–4363. doi: 10.1088/0031-9155/61/12/4346
- Reilly, J. P., and Diamant, A. M. (2011). *Electrostimulation: Theory, Applications, and Computational Model*. Boston: Artech House.
- Sasaki, K., Wake, K., and Watanabe, S. (2016). Conductivities of epidermis, dermis and subcutaneous tissue at intermediate frequencies. *Phys. Med. Biol.* 61, 4376–4389. doi: 10.1088/0031-9155/61/12/4376
- Schmid, G., Cecil, S., and  berbacher, R. (2013). The role of skin conductivity in a low frequency exposure assessment for peripheral nerve tissue according to the ICNIRP 2010 guidelines. *Phys. Med. Biol.* 58, 4703–4716. doi: 10.1088/0031-9155/58/13/4703
- Suzuki, Y., Muramatsu, K., Maruo, K., Kato, H., Tanabe, Y., Tubaki, T., et al. (2020). Pain thresholds are unaffected by age in a Japanese population. *Muscle Nerve* 61, 653–656. doi: 10.1002/mus.26834
- Sweeney, J., Mortimer, J., and Durand, D. (1987). “Modeling of mammalian myelinated nerve for functional neuromuscular stimulation,” in *Proceedings of the IEEE 9th Annual Conference of the Engineering in Medicine and Biology Society*, New York, NY.
- Tigerholm, J., Poulsen, A. H., Andersen, O. K., and Mørch, C. D. (2019). From perception threshold to ion channels—a computational study. *Biophys. J.* 117, 281–295. doi: 10.1016/j.bpj.2019.04.041
- Valentin, J. (2002). Basic anatomical and physiological data for use in radiological protection: reference values: ICRP Publication 89. *Ann. ICRP* 32:277. doi: 10.1016/S0146-6453(03)00002-2
- Vallbo, A. B., Hagbarth, K., Torebjork, H., and Wallin, B. (1979). Somatosensory, proprioceptive, and sympathetic activity in human peripheral nerves. *Physiol. Rev.* 59, 919–957. doi: 10.1152/physrev.1979.59.4.919
- Yamamoto, T., and Yamamoto, Y. (1981). Non-linear electrical properties of skin in the low frequency range. *Med. Biol. Eng. Comput.* 19, 302–310. doi: 10.1007/BF02442549

**Conflict of Interest:** The authors declare that the research was conducted in the absence of any commercial or financial relationships that could be construed as a potential conflict of interest.

Copyright   2021 Tanaka, Gomez-Tames, Wasaka, Inui, Ueno and Hirata. This is an open-access article distributed under the terms of the Creative Commons Attribution License (CC BY). The use, distribution or reproduction in other forums is permitted, provided the original author(s) and the copyright owner(s) are credited and that the original publication in this journal is cited, in accordance with accepted academic practice. No use, distribution or reproduction is permitted which does not comply with these terms.